Available online at www.sciencedirect.com
ScienceDirect
Biochimica et Biophysica Acta 1778 (2008) 1213–1221
Biochimica et Biophysica Acta BBA
www.elsevier.com/locate/bbamem

Resonance energy transfer study of lysozyme–lipid interactions

Galyna P. Gorbenko [a,*], Valeriya M. Ioffe [a], Julian G. Molotkovsky [b], Paavo K.J. Kinnunen [c]

[a] Department of Biological and Medical Physics, V.N. Karazin Kharkiv National University, 4 Svobody Sq., Kharkiv 61077, Ukraine
[b] Shemyakin-Ovchinnikov Institute of Bioorganic Chemistry, Russian Academy of Sciences, 16/10 Miklukho-Maklaya, Moscow 117871, Russia
[c] Helsinki Biophysics and Biomembrane Group, Institute of Biomedicine, P.O. Box 63, Haartmaninkatu 8, University of Helsinki, FIN-00014, Finland

Received 14 June 2007; received in revised form 6 September 2007; accepted 17 September 2007
Available online 5 October 2007

Abstract

Resonance energy transfer (RET) between the tryptophan residues of lysozyme as donors and anthrylvinyl-labeled phosphatidylcholine (AV-PC) or phosphatidylglycerol (AV-PG) as acceptors has been examined to gain insight into molecular level details of the interactions of lysozyme with the lipid bilayers composed of PC with 10, 20, or 40 mol% PG. Energy transfer efficiency determined from the enhanced acceptor fluorescence was found to increase with content of the acidic lipid and surface coverage. The results of RET experiments performed with lipid vesicles containing 40 mol% PG were quantitatively analyzed in terms of the model of energy transfer in two-dimensional systems taking into account the distance dependence of orientation factor. Evidence for an interfacial location of the two predominant lysozyme fluorophores, Trp62 and Trp108, was obtained. The RET enhancement observed while employing AV-PG instead of AV-PC as an energy acceptor was interpreted as arising from the ability of lysozyme to bring about local demixing of the neutral and charged lipids in PC/PG model membranes.

Keywords: Resonance energy transfer; Lysozyme; Protein–lipid interaction; Tryptophan bilayer location; Lipid demixing

1. Introduction

Model systems containing isolated proteins and lipid vesicles of varying compositions have long been employed in elucidating fundamental aspects of interactions between these major membrane constituents [1–3]. One widely used model protein with well-characterized structure is lysozyme, which avidly interacts with lipids [4–9]. The lysozyme–membrane interaction involves several interrelated steps, viz. (i) protein adsorption on the membrane surface driven by electrostatic interactions between the oppositely charged amino acid side chains and phospholipid headgroups [10,11], (ii) modification of the membrane physical properties including, particularly, reduction of electrostatic surface potential [11], lipid dehydration [8], decrease of the bilayer free volume [12], (iii) destabilization of the protein structure accompanied by partial unfolding, increase of molecular flexibility and exposure of additional hydrophobic regions on the protein surface [13], (iv) insertion of the conformationally altered protein molecule into the membrane interior [1,6,10], and (v) oligomerization of the protein [14], eventually leading to the formation of amyloid fibers [15].

Lipid-binding properties of lysozyme are hypothesized to be essential for its biological functions including antimicrobial, antitumor, and immunomodulatory activities. More specifically, a mechanism of bactericidal action independent of lysozyme ability to hydrolyze peptidoglycan layer of the bacterial cell wall has been proposed [16–18]. Regarding this mechanism the antimicrobial activity of lysozyme is considered to correlate with its structural features, charge distribution and surface hydrophobicity. These features are thought to determine the extent of the protein insertion into lipid bilayer giving rise to membrane permeabilization and loss of viability of bacterial cells. A specific helix–loop–helix domain capable of penetrating into lipid phase has been identified [17,18].

Another important implication of lysozyme–lipid interactions involves a possibility of the protein self-assembly into fibrillar aggregates with a core cross-β-sheet structure in a membrane environment [15]. This type of protein aggregates currently attracts special interest because of its key role in the pathogenesis of the so-called conformational diseases [19]. Membrane-related factors favoring protein fibrillization are thought to include

* Corresponding author. 52-52 Tobolskaya Str., Kharkiv 61072, Ukraine.
E-mail address: galyna.p.gorbenko@univer.kharkov.ua (G.P. Gorbenko).

0005-2736/$ - see front matter © 2007 Elsevier B.V. All rights reserved.
doi:10.1016/j.bbamem.2007.09.027

protein accumulation at the oppositely charged lipid–water interface, membrane-induced changes in the conformation and charge state of the protein, and specific arrangement of the solvent exposed and bilayer-buried portions of polypeptide chain [20]. Variation in the depth of bilayer penetration is assumed to modulate the propensity of a protein to act as a nucleus in fibril formation [21].

In the light of the above gaining further insight into the structural details of lysozyme–lipid interactions seems to be of importance at least in two basic aspects concerning the structural prerequisites for both its bactericidal activity and aggregation behavior in a membrane environment. To this end, the present study was focused on obtaining structural information on the model systems containing lysozyme and lipid vesicles composed of zwitterionic phosphatidylcholine and anionic phosphatidylglycerol. To characterize these systems in terms of the protein location relative to lipid–water interface we examined resonance energy transfer (RET) between the tryptophan residues of lysozyme as donors and anthrylvinyl-labeled phosphatidylcholine (AV-PC) or anthrylvinyl-labeled phosphatidylglycerol (AV-PG) as acceptors. Comparison of energy transfer efficiencies for AV-PC and AV-PG allowed us to address the question of whether lysozyme is capable of inducing the formation of lateral domains enriched in acidic lipids.

2. Materials and methods

2.1. Chemicals

Chicken egg white lysozyme and HEPES were purchased from Sigma (St. Louis, MO, USA). 1-palmitoyl-2-oleoyl-*sn*-glycero-3-phosphocholine (PC) and 1-palmitoyl-2-oleoyl-*sn*-glycero-3-phospho-*rac*-glycerol (PG) were from Avanti Polar Lipids (Alabaster, AL). Fluorescent lipids, 1-acyl-2-[12-(9-anthryl)-11-trans-dodecenoyl]-*sn*-glycero-3-phosphocholine (AV-PC), and 1-acyl-2-[12-(9-anthryl)-11-trans-dodecenoyl]-*sn*-glycero-3-phospho-1-*rac*-glycerol (AV-PG) were synthesized as described in detail elsewhere [22,23]. All other chemicals were of analytical grade.

2.2. Preparation of lipid vesicles

Large unilamellar vesicles were prepared by extrusion from PC mixtures with PG (10, 20 or 40 mol%). A thin lipid film was first formed from the lipid mixtures in chloroform by removing the solvent under a stream of nitrogen. The dry lipid residues were subsequently hydrated with 20 mM HEPES, 0.1 mM EDTA, pH 7.4 at room temperature to yield lipid concentration of 1 mM. Thereafter, the sample was subjected to 15 passes through a 100 nm pore size polycarbonate filter (Millipore, Bedford, USA), yielding liposomes of desired composition. AV-PC or AV-PG (maximum 1.5 mol% of total lipid) were added to the mixture of PC and PG prior to the solvent evaporation. The concentration of fluorescent lipid was determined spectrophotometrically using anthrylvinyl extinction coefficient $E_{367}=9\times10^3$ M^{-1} cm^{-1} [22].

To evaluate pH dependence of RET efficiency, fluorescently-labelled liposomes were prepared using 20 mM phosphate (pH 6.2) and acetate (pH 3.7) buffers instead of HEPES.

2.3. Fluorescence measurements

Fluorescence measurements were performed at 25 °C using 10 mm pathlength quartz cuvettes with spectrofluorometer equipped with a magnetically stirred, thermostated cuvette holder (LS-50B, Perkin-Elmer Ltd., Beaconsfield, UK). Emission spectra of AV-labeled phospholipids were recorded at excitation wavelength of 296 nm with excitation and emission band passes set at 10 nm. While recording AV excitation spectra emission wavelength was 430 nm and both band passes set at 5 nm. The efficiency of energy transfer was calculated from the sensitized emission of the acceptor [24]:

$$E = \frac{A_A(\lambda_D^{ex})}{A_D(\lambda_D^{ex})}\left[\frac{I_{AD}(\lambda_A^{em})}{I_A(\lambda_A^{em})} - 1\right] \quad (1)$$

where $A_{A,D}$ are the optical densities of the acceptor (AV) and donor (Trp) at the donor excitation wavelength $\lambda_D^{ex} = 296$ nm, I are the acceptor fluorescence intensities measured at the acceptor emission wavelength ($\lambda_A^{em} = 430$ nm) in the absence (I_A) and presence (I_{AD}) of the donor. Fluorescence intensities measured in the presence of lysozyme at the maximum of AV-PC or AV-PG emission spectra (430 nm) were corrected for inner filter effects using the following coefficients [25]:

$$k_{corr} = \frac{(1-10^{-A_A(\lambda_D^{ex})})(A_A(\lambda_D^{ex}) + A_D(\lambda_D^{ex}))}{(1-10^{-(A_A(\lambda_D^{ex})+A_D(\lambda_D^{ex}))})A_A(\lambda_D^{ex})} \quad (2)$$

Steady-state fluorescence anisotropy of AV fluorophore was measured at excitation and emission wavelengths of 296 and 430 nm, respectively, with excitation and emission band passes set at 10 nm.

2.4. Theory

The results of RET measurements have been quantitatively interpreted in terms of the model of energy transfer on a surface formulated by Fung and Stryer [26] and extended in our previous studies [27] to allow for distance dependence of orientation factor in two-dimensional systems. Assuming that donors and acceptors are randomly distributed in different planes separated by a distance d_a, the efficiency of energy transfer is given by:

$$E = 1 - \int_0^\infty \exp(-\lambda)\exp(-C_a^s S(\lambda))d\lambda \quad (3)$$

$$S(\lambda) = \int_{d_a}^\infty \left[1 - \exp\left(-\lambda\left(\frac{R_o}{R}\right)^6\right)\right] 2\pi R dR \quad (4)$$

where $\lambda = t/\tau_d$, τ_d is the lifetime of excited donor in the absence of acceptor, R_o is the Förster radius, C_a^s is the concentration of acceptors per unit area related to the molar concentrations of the fluorescent lipids (L_{AV}) and total lipids (L_o):

$$C_a^s = \frac{L_{AV}}{L_o(f_{PC}S_{PC} + f_{PG}S_{PG})} \quad (5)$$

here f, S are the mole fractions and mean areas per PC or PG molecule taken as $S_{PC}=S_{PG}=S_L=0.65$ nm^2. Förster radius is known to depend on the donor quantum yield (Q_D) and the overlap between the donor emission ($F_D(\lambda)$) and acceptor absorption ($\varepsilon_A(\lambda)$) spectra:

$$R_o = 979(\kappa^2 n_r^{-4} Q_D J)^{1/6}; \quad J = \frac{\int_0^\infty F_D(\lambda)\varepsilon_A(\lambda)\lambda^4 d\lambda}{\int_0^\infty F_D(\lambda)d\lambda} \quad (6)$$

where n_r is the refractive index of the medium ($n_r=1.37$), κ^2 is an orientation factor defined as [24]:

$$\kappa^2 = (\sin\theta_D \sin\theta_A \cos\phi - 2\cos\theta_D \cos\theta_A)^2 \quad (7)$$

where θ_D and θ_A are the angles between the donor emission (***D***) or acceptor absorption (***A***) transition moments and the vector ***R*** joining the donor and acceptor, ϕ is the dihedral angle between the planes (***D***, ***R***) and (***A***, ***R***).

The applicability of Eq. (7) is limited to the case where the vectors ***D*** and ***A*** do not undergo any reorientation during the transfer time. Alternatively, Förster radius should be calculated using the dynamic average value of orientation

factor ($\langle\kappa^2\rangle$). If the donor emission and acceptor absorption transition moments are symmetrically distributed within the cones about certain axes $\boldsymbol{D_x}$ and $\boldsymbol{A_x}$, $\langle\kappa^2\rangle$ is given by [28]:

$$\langle\kappa^2\rangle = (\sin\Theta_D\sin\Theta_A\cos\Phi - 2\cos\Theta_D\cos\Theta_A)^2\langle d_D^x\rangle\langle d_A^x\rangle + 1/3(1-\langle d_D^x\rangle) + 1/3(1-\langle d_A^x\rangle) + \cos^2\Theta_D\langle d_D^x\rangle(1-\langle d_A^x\rangle) + \cos^2\Theta_A\langle d_A^x\rangle(1-\langle d_D^x\rangle) \quad (8)$$

where Θ_D and Θ_A are the angles made by the axes $\boldsymbol{D_x}$ and $\boldsymbol{A_x}$ with the vector $\boldsymbol{R}$, Φ is the angle between the planes containing the cone axes and the vector $\boldsymbol{R}$, $\langle d_D^x\rangle$ and $\langle d_A^x\rangle$ are so-called axial depolarization factors:

$$\langle d_{D,A}^x\rangle = 3/2\langle\cos^2\psi_{D,A}\rangle - 1/2 \quad (9)$$

where $\Psi_{D,A}$ are the cone half-angles. These factors are related to the steady-state (r) and fundamental (r_0) anisotropies of donor and acceptor [28]:

$$d_{D,A}^x = \pm(r_{D,A}/r_{0D,A})^{1/2} \quad (10)$$

When the donor and acceptor planar arrays are located at different levels across the membrane multiple donor–acceptor pairs are involved in energy transfer, so that orientation factor appears to be a function of the donor–acceptor separation (R). Particularly, for the most probable membrane orientation of $\boldsymbol{D_x}$ and $\boldsymbol{A_x}$, parallel to the bilayer normal, the angles Θ_D and Θ_A made by $\boldsymbol{D_x}$ and $\boldsymbol{A_x}$ with $\boldsymbol{R}$ are equal and depend on the distance between donor and acceptor ($\Theta_A=\Theta_D=\theta$, $\theta=f(R)$). Under these circumstances Eq. (8) can be rewritten in the form:

$$\langle\kappa^2(\theta)\rangle = \langle d_D^x\rangle\langle d_A^x\rangle(3\cos^2\theta-1)^2 + 1/3(1-\langle d_D^x\rangle) + 1/3(1-\langle d_A^x\rangle) + \cos^2\theta(\langle d_D^x\rangle - 2\langle d_D^x\rangle\langle d_A^x\rangle + \langle d_A^x\rangle) \quad (11)$$

where $\cos^2\theta=(d_a/R)^2$. Next, by representing Förster radius as $R_0=[\kappa^2(R)]^{1/6}\ R_0^r$ one obtains:

$$S(t) = \int_{d_a}^{\infty}\left[1-\exp\left(-\lambda\kappa^2(R)\left(\frac{R_o^r}{R}\right)^6\right)\right]2\pi R dR; \quad R_o^r = 979\left(n_r^{-4}Q_D J\right)^{1/6} \quad (12)$$

In analyzing the RET data presented here we considered the lipid–protein systems as containing one donor plane located at a distance d_c from the membrane center and two acceptor planes separated by a distance d_t (Fig. 1)). Given that for the outer acceptor plane $d_a=|d_c-0.5d_t|$ while for the inner plane $d_a=d_c+0.5d_t$, the following relationships hold:

$$S_1(\lambda) = \int_{|d_c-0.5d_t|}^{\infty}\left[1-\exp\left(-\lambda\kappa_1^2(R)\left(\frac{R_o^r}{R}\right)^6\right)\right]2\pi R dR \quad (13)$$

$$S_2(\lambda) = \int_{d_c+0.5d_t}^{\infty}\left[1-\exp\left(-\lambda\kappa_2^2(R)\left(\frac{R_o^r}{R}\right)^6\right)\right]2\pi R dR \quad (14)$$

$$\kappa_{1,2}^2(R) = \langle d_D^x\rangle\langle d_A^x\rangle\left(3\left(\frac{d_c\mp0.5d_t}{R}\right)^2-1\right) + \frac{1-\langle d_D^x\rangle}{3} + \frac{1-\langle d_A^x\rangle}{3} + \left(\frac{d_c\mp0.5d_t}{R}\right)^2\left(\langle d_D^x\rangle - 2\langle d_D^x\rangle\langle d_A^x\rangle + \langle d_A^x\rangle\right) \quad (15)$$

$$E = 1 - \int_0^{\infty}\exp(-\lambda)\exp\left[-C_a^s(S_1(\lambda)+S_2(\lambda))\right]d\lambda \quad (16)$$

where S_1 and S_2 are the quenching contributions describing energy transfer to the outer and inner acceptor planes, respectively. The relationships (13)–(16) are valid when the donor and acceptor transition moments are distributed about the axes $\boldsymbol{D_x}$ and $\boldsymbol{A_x}$ parallel to the bilayer normal $\boldsymbol{N}$. If this is not the case, additional depolarization factors accounting for the deviations of $\boldsymbol{D_x}$ and $\boldsymbol{A_x}$ from $\boldsymbol{N}$ should be introduced: $d_{D,A}^a = \frac{3}{2}\cos^2\alpha_{D,A} - \frac{1}{2}$, where $\alpha_{D,A}$ are the angles made by $\boldsymbol{D_x}$ and $\boldsymbol{A_x}$ with $\boldsymbol{N}$. By applying the Soleillet's theorem stating the multiplicativity of depolarization factors, Eq. (15) may be rewritten in a more general form:

$$\kappa_{1,2}^2(R) = d_D d_A\left(3\left(\frac{d_c\mp0.5d_t}{R}\right)^2-1\right) + \frac{1-d_D}{3} + \frac{1-d_A}{3} + \left(\frac{d_c\mp0.5d_t}{R}\right)^2(d_D - 2d_D d_A + d_A) \quad (17)$$

where $d_{D,A}=\langle d_{D,A}^x\rangle d_{D,A}^a$

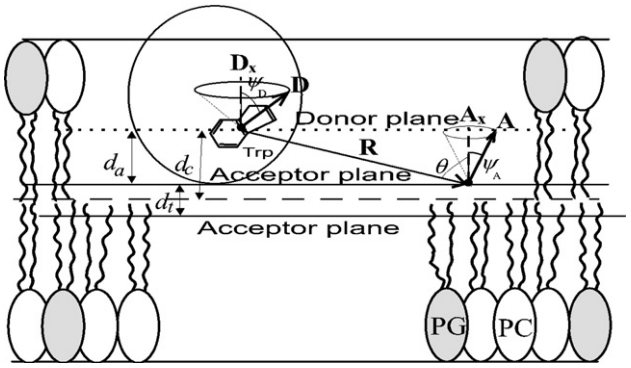

Fig. 1. Schematic representation for relative bilayer positions and angular relationships of donors (Trp residues of lysozyme) and acceptors (anthrylvinyl moiety of AV-PC or AV-PG) in the model membranes.

Acyl bearing AV fluorophore, 12-(9-anthryl)-11-*trans*-dodecenoyl, has no polar group in its chain; being fully immersed in the hydrophobic core of a lipid bilayer, as judged from ^{1}H-NMR-spectroscopy data [23] and quenching of AV fluorescence by iodide [29]. ^{1}H-NMR measurements revealed that AV-PC induces upfield shift of the proton resonances at the level of terminal CH_3 groups and C4-C13 methylenes, exerting no effect on the resonances of choline protons [23]. This observation provides strong support to the idea that AV fluorophore is localized in a lipid bilayer close to the terminal methyl groups, preferentially orienting parallel to acyl chains. In the above RET model the spatial relationships between the donors and acceptors are defined by the parameters d_c and d_t, characterizing the distance between the donor plane and membrane center, and separation between the outer and inner acceptor planes, respectively. The former parameter was optimized while the latter was taken from the limits consistent with the size of AV fluorophore (ca. 0.7×0.3 nm) and the above assumption concerning the AV bilayer location. In addition, allowing for the high mobility of the terminal groups of hydrocarbon chains, it seemed reasonable to take d_t value from the range 0.3–0.7 nm.

Notably, varying the parameter d_t from the lower (0.3 nm) to upper (0.7 nm) limits yielded d_c increase not exceeding 0.1 nm, indicating that the results of data treatment in terms of the above RET model slightly depend on the uncertainty in the AV bilayer location.

3. Results

The efficiency of energy transfer is typically determined by monitoring a decrease in the donor quantum yield in the presence of an acceptor [24]. Unfortunately, this method appeared inapplicable to the protein–lipid systems under study because of lysozyme causing aggregation and fusion of lipid vesicles [4–7]. Within the ranges of lysozyme and lipid concentrations where aggregation and fusion did not occur (as judged by light scattering measurements) we did not observe any significant changes in tryptophan emission upon the binding of lysozyme to membranes.

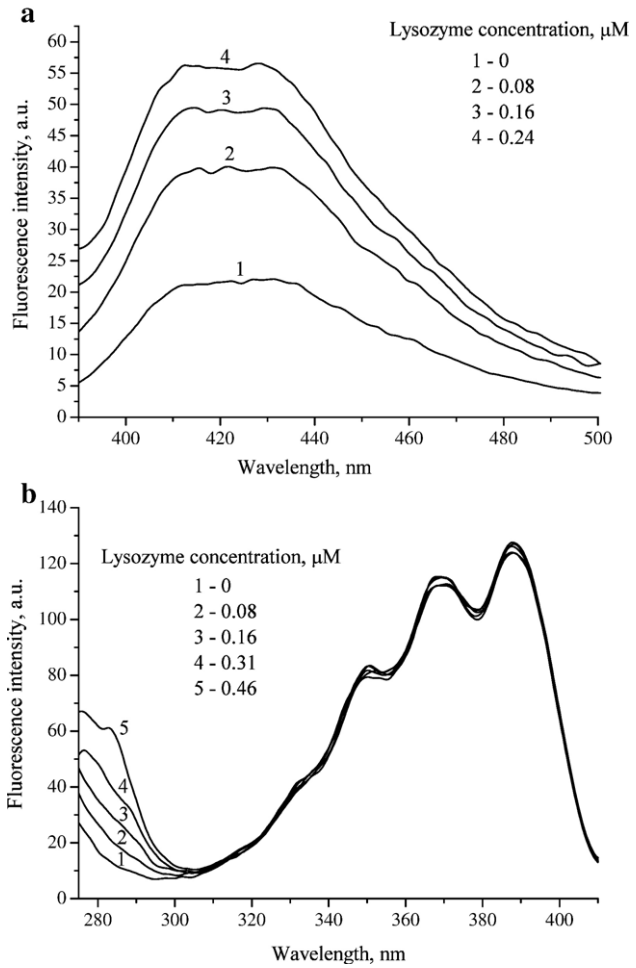

Fig. 2. Emission (a) and excitation (b) spectra of AV-PC in PC/PG liposomes (40 mol% PG) recorded at varying lipid-to-protein molar ratio. Lipid concentration was 5 μM (a) or 10 μM (b).

It seems likely that the quenching of Trp fluorescence by AV fluorophore is balanced by the contributions of free protein and directly excited acceptors to the measured fluorescence intensity. To circumvent this problem, we tried to detect RET by another method based on enhancement of acceptor fluorescence due to energy transfer from a donor. Accordingly, we monitored the membrane association of lysozyme upon its addition to liposomes containing AV-PC by measuring the increase in AV fluorescence (Fig. 2a). It could be assumed that the observed enhancement of AV emission arises from direct effect of the protein on acceptor fluorescence, for instance, through rigidifying the acyl chain groups in the fluorophore surroundings. However, in this case it is difficult to explain increasing magnitude of lysozyme-induced effect with acceptor concentration. Although the molar fraction of AV-lipids is varied, proportions of PG or PC remain constant, so that the amount of bound protein, and, as a consequence, the extent of bilayer modification, seems hardly to depend on AV concentration. Likewise, the finding that fluorescence changes are different for AV-PC and AV-PG-containing systems with the same PG mole fraction (vide infra), could hardly be rationalized in terms of a direct effect of lysozyme on the acceptor fluorescence. All these considerations led us to conclude that Trp residues of lysozyme serve as energy donors for AV acceptors.

Additional proof of energy transfer from Trp to AV comes from the observation that the intensity of acceptor excitation spectra at the donor absorption wavelengths increases with increasing protein concentration (Fig. 2b). Since lysozyme is a multi-tryptophan protein a question arises which residues may participate in energy transfer to AV-acceptor. There are six tryptophan residues in lysozyme molecule, three of which (Trp62, Trp63 and Trp108) are located in the active site and exposed to a solvent, while Trp28 and Trp111 reside in a hydrophobic environment. Notably, 80% of lysozyme fluorescence has been assigned to Trp62 and Trp108 with a possibility of energy migration from Trp 108 to Trp62 [30,31]. In view of this, in the analyses given below the two dominant emitters, Trp62 and Trp 108, were regarded as energy donors for AV acceptors.

The efficiency of energy transfer calculated from the enhanced acceptor emission using the Eq. (1) was found to depend on both protein and lipid concentration, as well as on the content of the acidic lipid in membranes. As demonstrated in Fig. 3a, at the highest employed acceptor concentration (1.5 mol%) this

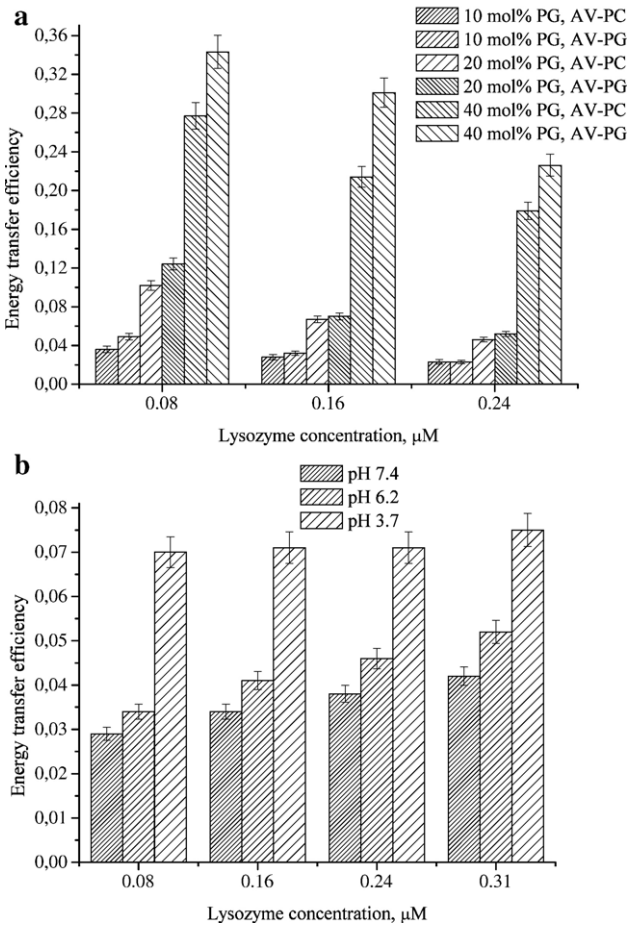

Fig. 3. Efficiency of energy transfer between lysozyme Trp residues and AV-PC or AV-PG measured at pH 7.4 (acceptor concentration 1.5 mol%) at varying membrane composition (a) and pH (b), 40 mol% PG, 1.5 mol% AV-PC. Lipid concentration was 5 μM (a) or 25 μM (b).

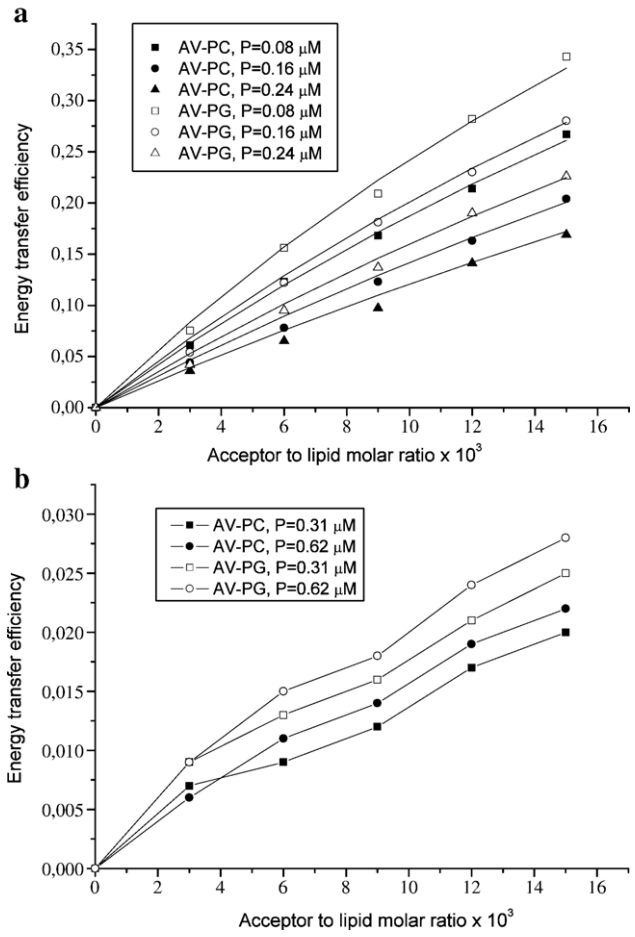

Fig. 4. Efficiency of energy transfer measured for PC/PG liposomes (40 mol% PG) as a function of acceptor to lipid molar ratio at lipid concentration 5 μM (a) or 50 μM (b). Solid lines represent theoretical curves providing the best fit of the model (Eqs. (13)–(17)) to the experimental data ($\alpha_D = \pi/2, +d_a, +d_D$).

quantity increased from ~2–4% to ~20–30% upon increasing the content of PG from 10 to 40 mol%. The use of AV-PG instead of AV-PC as an energy donor in membranes containing 40 mol% PG resulted in higher RET efficiencies (Fig. 4a), suggesting the enrichment of PG in the protein binding site. Likewise, RET enhancement was observed upon decreasing lipid concentration coupled with increased surface coverage (cf. Fig. 4a and b) and lowering of pH (Fig. 3b).

The results of RET measurements were quantitatively analyzed within the framework of the above theoretical model. This analysis was restricted to lipid vesicles containing 40% PG, because only in this case RET efficiencies were sufficiently high for obtaining quantitative estimates. First, the RET data were treated assuming that donors and acceptors are randomly distributed in separate parallel planes. The fitting of theoretical model given by Eqs. (13)–(17) to the experimental dependencies of RET efficiency on acceptor to lipid molar ratio (Fig. 4a) allowed us to evaluate the distance between the donor plane and bilayer center (d_c). Notably, we consider this parameter as being averaged over bilayer positions of both predominant lysozyme fluorophores, Trp62 and Trp108. The value of d_c was estimated by nonlinear least-squares technique involving minimization of the following error function:

$$\chi^2 = \frac{\sum_{i=1}^{n} (E_{ei} - E_{ci})^2}{n} \quad (18)$$

where n is the number of experimental points (*i.e.*, the number of acceptor concentrations), E_e is the measured transfer efficiency, E_c is the transfer efficiency calculated by numerical integration of the Eqs. (13)–(17). The data fitting procedure yielded χ^2 values not exceeding 1.6×10^{-4}.

The axial depolarization factors $\langle d_D^x \rangle$ and $\langle d_A^x \rangle$ were calculated from Eq. (10) using the results of steady-state fluorescence anisotropy measurements. We failed to detect any significant changes in tryptophan fluorescence anisotropy upon the transfer of lysozyme from the solution to the membrane surface. This parameter (r_D) measured with $\lambda_{ex}=296$ nm and $\lambda_{em}=338$ nm was found to be ~0.1. The anisotropy of AV-PC and AV-PG (r_A) tended to increase with the protein concentration (Fig. 5)). The fundamental anisotropy of anthrylvinyl fluorophore (r_{oA}) was reported to be ~0.08 at $\lambda_{ex}=296$ nm [32]. The tryptophan absorbance in the range 250–300 nm is known to originate from the two electronic transitions ^1L_a and ^1L_b whose transition moments are orthogonally oriented [33]. Excitation wavelength of 296 nm employed in the RET experiments described here predominantly populates the ^1L_a state of the fluorophore with $r_{oD}=0.3$ [24]. The transition moment of this state lies in the plane of the indole ring [34], so that the angle α_D reflects the deviation of the normal to the plane of the Trp aromatic ring from the bilayer normal. Based on the available experimental evidence we could not make any assumptions about preferable orientation of the Trp residues in lipid-bound lysozyme. Therefore, the RET curves were analyzed with the two limiting assumptions of $\alpha_D=0$ (the plane of indole ring parallel to the bilayer surface) and $\alpha_D=\pi/2$ (the plane of indole ring perpendicular to the bilayer surface).

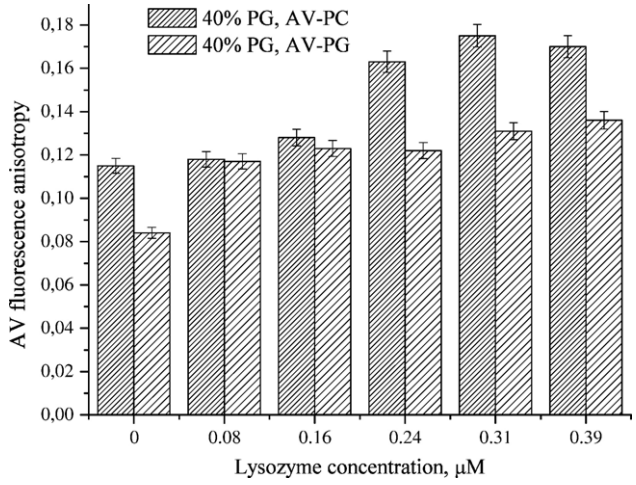

Fig. 5. AV fluorescence anisotropy measured with $\lambda_{ex}=296$ nm and $\lambda_{em}=430$ nm for different lipid-to-protein molar ratios. Lipid concentration was 5 μM, acceptor concentration 1.5 mol%.

As indicated above, the anthrylvinyl moiety linked to the end of acyl chains adopts preferential orientation parallel to the bilayer normal [23]. This allowed us to put α_A equal to $\pi/2$. Allowing for the possibility of both positive and negative values of $\langle d_D^x \rangle$ and $\langle d_A^x \rangle$ (see Eq. (10)) all possible combinations of the signs of these parameters were considered in the data fitting.

4. Discussion

Presented in Table 1 are the estimates for d_c recovered from systems containing AV-PC (d_c^{APC}) or AV-PG (d_c^{APG}) while assuming randomly distributed donors and acceptors. If this assumption was valid there would be no differences between the RET curves obtained using either AV-PC or AV-PG as energy acceptors. The finding that energy transfer to AV-PG is more effective (Fig. 4a) compared to AV-PC can be interpreted as arising from lipid lateral redistribution which is followed by accumulation of acidic lipids in the vicinity of bound protein. As the positively charged lysozyme approaches the membrane surface PG molecules are allowed to migrate toward interaction zone, thereby replacing PC molecules. In view of the exchange between the charged and neutral lipids the assumption about random acceptor distribution would lead to d_c overestimates for the systems with AV-PC and d_c underestimates for the systems with AV-PG. Accordingly, true d_c value might be expected to lie between d_c^{APG} and d_c^{APC}.

The limiting values thus obtained for d_c are consistent with the location of lysozyme Trp residues in the interfacial bilayer region composed of phosphorylcholine moiety ($d_c \sim 2$–2.2 nm), glycerol backbone ($d_c \sim 1.7$–1.8 nm), carbonyls ($d_c \sim 1.4$–1.5 nm), upper acyl chain carbons ($d_c \sim 1.3$ nm) and hydration water. This finding supports the notion that tryptophan residues of membrane-bound peptides and proteins tend to reside at lipid–water interface [3,35]. Such a preference is supposed to be associated with Trp propensity for dipolar, cation- π and hydrogen bonding interactions with interfacially located lipid structural groups. Additionally, our data agree with the viewpoint that helix–loop–helix domain (87–114 residues of hen egg white lysozyme) located at the upper lip of the active site cleft accounts for lysozyme insertion into lipid bilayer [18]. The nonpolar portion of this domain (residues 87–95) penetrating into hydrophobic bilayer region serves as a membrane anchor, while terminal basic residues form electrostatic contacts with anionic phospholipid headgroups. This mode of membrane binding of lysozyme causes Trp62 and Trp108 to be accommodated in the interface. Hence, our RET-based estimates on the bilayer location of Trp residues may be regarded as additional evidence for the ability of lysozyme to insert into the lipid phase. Evidence in favour of the involvement of hydrophobic interactions in the association of with membranes have been obtained using fluorescence polarization [6], vesicle leakage [1,6] and monolayer [10] experiments. Notably, our observation that RET efficiency increases at lower pH (Fig. 3b) is in keeping with the early [5] and recent [10] findings suggesting that acidic pH favors the penetration of lysozyme into the bilayer. Although lysozyme is a very stable protein whose structure in solution remains virtually unperturbed on pH shift from the neutral to acidic values [36], it seems highly probable that formation of ionic and hydrophobic contacts with lipid molecules could modulate the pH sensitivity of this protein.

As the next step of data analysis we assessed the magnitude of the lysozyme-induced lipid redistribution manifesting as the difference between AV-PC and AV-PG-containing systems in the RET efficiencies. The effects of lateral redistribution of anionic and neutral lipids in response to the binding of basic peptide or protein have been scrutinized, both theoretically and experimentally, in a number of studies [37–41]. Theoretical models for this phenomenon have been proposed by Mosior and McLaughlin [37], Denisov et al. [38], Heimburg et al. [39], May et al. [40], Mbamala et al. [41]. Two underlying processes are considered, viz. (i) local lipid demixing implicating molecular scale deviation from the average lipid composition within and around the protein–membrane interaction zone, and (ii) the formation of macroscopic protein–lipid domains enriched in acidic lipids. The extent of lipid demixing is thought to be dictated by the minimum of the total interaction free energy reflecting the balance between the gain in electrostatic adsorption energy and the loss of lipid mixing entropy. The models for domain formation emphasize the importance of both electrostatic [38] and nonelectrostatic [40,42] mechanisms. The latter involves lipid-mediated attraction between adsorbed proteins coupled with elastic membrane deformation [40,41]. Experimentally, lipid redistribution has been observed for instance in the adsorption of cytochrome *c* [43], carditoxin II [44],

Table 1
Tryptophan distance from the center of PC/PG bilayer (40 mol% PG) in lysozyme–lipid systems containing AV-PC (d_c^{APC}, nm) or AV-PG (d_c^{APC}, nm) as energy acceptors

Protein concentration, μM	d_c^{APC}, $\alpha_D = \pi/2$				d_c^{APC}, $\alpha_D = 0$		d_c limits, nm
	$+d_A, +d_D$	$+d_A, -d_D$	$-d_A, +d_D$	$-d_A, -d_D$	$+d_A, -d_D$	$-d_A, +d_D$	
0.08	1.8 (9.6×10^{-5})	2.0 (9.8×10^{-5})	2.1 (9.7×10^{-5})	2.2 (8.5×10^{-5})	1.6 (9.5×10^{-5})	2.2 (8.1×10^{-5})	1.6–2.2
0.16	2.0 (6.1×10^{-5})	2.2 (6.4×10^{-5})	2.4 (6.3×10^{-5})	2.5 (5.8×10^{-5})	1.8 (5.9×10^{-5})	2.6 (5.6×10^{-5})	1.8–2.6
0.24	2.1 (7.0×10^{-5})	2.4 (7.6×10^{-5})	2.6 (7.1×10^{-5})	2.7 (6.8×10^{-5})	1.9 (6.7×10^{-5})	2.7 (6.7×10^{-5})	1.9–2.7
	d_c^{APG}, $\alpha_D = \pi/2$				d_c^{APG}, $\alpha_D = 0$		
0.08	1.6 (6.4×10^{-5})	1.8 (6.5×10^{-5})	1.9 (6.1×10^{-5})	1.8 (4.9×10^{-5})	1.4 (6.8×10^{-5})	1.7 (4.4×10^{-5})	1.4–1.9
0.16	1.7 (1.5×10^{-4})	2.0 (1.5×10^{-4})	2.1 (1.6×10^{-4})	2.1 (1.4×10^{-4})	1.5 (1.6×10^{-4})	2.0 (1.4×10^{-4})	1.5–2.1
0.24	1.9 (6.9×10^{-5})	2.2 (7.1×10^{-5})	2.3 (7.0×10^{-5})	2.4 (6.5×10^{-5})	1.7 (6.7×10^{-5})	2.4 (6.3×10^{-5})	1.7–2.4

Shown in parentheses are χ^2 values for each data fit. Error of d_c estimation did not exceed 0.2 nm.

polylysine [45] and basic peptides [46] to negatively charged model membranes.

The RET data presented here are suggestive of ability of lysozyme to produce the deviation of PG concentration from its bulk value in the membrane–protein interaction zone. The simplest way by which this process can be allowed for in the above RET model involves introducing the additional parameters, characterizing the size of interaction zone (r_{dm}), the ratio of PG concentrations in the interaction zone at nonrandom and random acceptor distribution (k) and the fraction of bound protein ($f_b = B/P$, where B is the molar concentration of bound protein and P is the total protein concentration). Thus, the expressions for RET efficiency take the form:

$$S_{11}(\lambda) = \int_{[r_{dm}^2+(d_c-0.5d_t)^2]^{0.5}}^{\infty} \left[1- \exp\left(-\lambda\kappa_1^2(R)\left(\frac{R_0^r}{R}\right)^6\right)\right] 2\pi R dR \quad (19)$$

$$S_{12}(\lambda) = \int_{|d_c-0.5d_t|}^{[r_{dm}^2+(d_c-0.5d_t)^2]^{0.5}} \left[1- \exp\left(-\lambda\kappa_1^2(R)\left(\frac{R_o^r}{R}\right)^6\right)\right] 2\pi R dR \quad (20)$$

$$E = 1 - \int_0^{\infty} \exp(-\lambda) \exp \times \left[- C_a^s \left(\left[\frac{L_{out}S_L - Pf_b\pi r_{dm}^2 k}{L_{out}S_L - Pf_b\pi r_{dm}^2}\right] S_{11}(\lambda) + kS_{12}(\lambda) + S_2(\lambda)\right)\right] d\lambda \quad (21)$$

where L_{out} is the lipid concentration in the outer monolayer.

The RET profiles obtained with AV-PG as energy acceptor were approximated by Eqs. (19)–(21), with k being varied from 1 to its maximum possible value (2.5) at 40 mol% PG. Parameter r_{dm} was taken from the limits dictated by the requirement $Pf_b\pi r_{dm}^2 k \le L_{out}S_L$, while parameter d_c was optimized. By analyzing the RET data in this manner we found good agreement between the theory and experiment under conditions where the size of the zone with increased PG concentration (r_{dm}) does not exceed 3.4 nm (Fig. 6). This value is comparable with the protein radius (ca. 3 nm) suggesting that lysozyme causes a local deviation from the average lipid composition.

The RET data presented here give also some grounds for believing that the mode of lysozyme–membrane association depends on surface coverage. As seen in Fig. 4b, at lipid concentration $L = 50$ μM the measured RET efficiencies were at the level of experimental error (ca. 3%), while a tenfold decrease of L value resulted in a marked enhancement of energy transfer (Fig. 4a). This phenomenon could be interpreted in terms of shallow location of electrostatically-bound lysozyme at relatively low surface coverage (L_{out}/P ratios greater than ~40) followed by

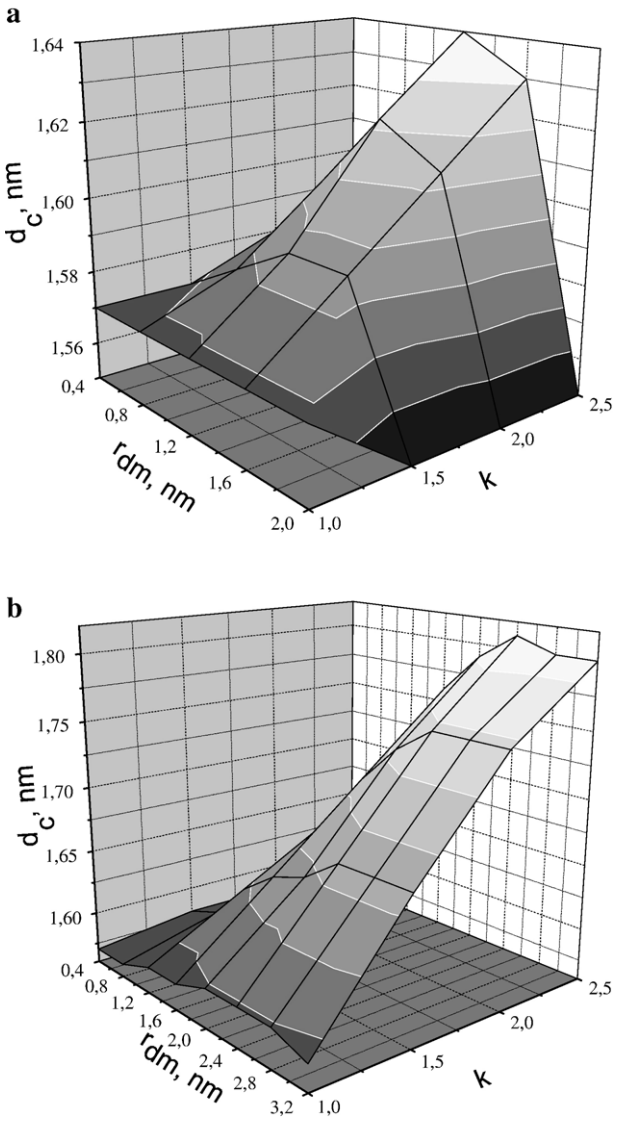

Fig. 6. Three-dimensional plots illustrating the relationships between the Trp distance from the bilayer center (d_c), radius of the protein–membrane interaction zone (r_{dm}) and a factor by which PG mole fraction increases in the interaction zone (k). The sets of parameters d_c, k, r_{dm} providing good agreement between theory and experiment ($5\times10^{-5} < \chi^2 < 7\times10^{-5}$) were obtained on the assumption of complete (a, $f_b = 1$) or incomplete (b, $f_b = 0.5$) protein binding.

the penetration of a certain fragment of polypeptide chain into the membrane interior when the surface coverage is becoming high enough to overcome the energy barrier for the protein insertion into the lipid phase. Importantly, coverage-dependent changes in the transverse bilayer location have been demonstrated in several recent studies for cytochrome c, another basic protein similar to lysozyme in its physicochemical properties [47,48]. By analogy with the so-called carpet mechanism proposed for peptide–membrane binding it was hypothesized that protein insertion into lipid bilayer is triggered by a certain critical surface coverage at which lateral pressure of two-dimensional adsorbate gas reaches its threshold value [49]. Given that lysozyme molecule represents a spheroid with dimensions 4.5 × 3 × 3 nm and cross-section ca. 13.5 nm^2 and taking molecular area per phospholipid headgroup

as 0.65 nm^2 it follows that theoretical saturation coverage of the membrane surface with lysozyme corresponds to L_{out}/P ratio of ca. 20. This value falls into the range of L_{out}/P ratios at which we succeeded in detecting energy transfer. It is noteworthy in this regard that at the protein and lipid concentrations employed in the RET experiments nearly complete binding of lysozyme to lipid vesicles containing 40 mol% PG might be expected. This is based on our binding studies performed with fluorescein-labeled lysozyme which, despite having somewhat lower affinity for lipids, showed virtually full transition into lipid-bound state under analogous experimental conditions [14]. Moreover, the experiments with the labeled protein led us to assume that within certain strictly defined ranges of the P and L values there exists an equilibrium between the monomeric and oligomeric species of membrane-associated lysozyme. In view of this possibility the diminished RET efficiency observed upon increasing lysozyme concentration (Fig. 4a) could be attributed to self-association of a certain fraction of the bound protein.

Clearly, processes such as protein aggregation in a membrane environment or lipid demixing give rise to nonrandom distribution of donors and acceptors. In this case extraction of adequate structural information from the RET experiments requires global data analysis using simulation-based fitting. However, allowing for the aforementioned complications in RET detection in lysozyme–lipid systems and limited number of RET measurements we found it reasonable to perform simplified analysis of the RET data as a first approximation to real situation.

In conclusion, the present RET study revealed three important features of lysozyme–lipid interactions. First, lysozyme location relative to lipid–water interface depends on surface coverage, as judged from the enhancement of resonance energy transfer between tryptophan residues of the protein and anthrylvinyl-labeled PC or PG on increasing protein surface density. Second, at lipid-to-protein molar ratios close to saturation surface coverage ($L_{out}/P \sim 20$, $L/P \sim 40$) partial insertion of lysozyme into PC/PG lipid bilayer (40 mol% PG) takes place, with predominant fluorophores Trp62 and Trp108 being located in the interfacial bilayer region. Third, lysozyme is capable of inducing lipid demixing in PC/PG membranes, as follows from the increase of PG mole fraction in the protein–membrane interaction zone. Importantly, all these characteristics of the adsorption of lysozyme to lipid membranes may also be relevant to its bactericidal and amyloidogenic properties.

Acknowledgements

GG gratefully acknowledges a visiting scientist award by the Sigrid Juselius Foundation. HBBG is supported by the Finnish Academy and Sigrid Juselius Foundation.

References

[1] H.K. Kimelberg, Protein–liposome interactions and their relevance to the structure and function of cell membranes, Mol. Cell. Biochem. 10 (1976) 171–190.
[2] P.K.J. Kinnunen, A. Koiv, J.Y.A. Lehtonen, M. Rytomaa, P. Mustonen, Lipid dynamics and peripheral interactions of proteins with membrane surfaces, Chem. Phys. Lipids 73 (1994) 181–207.
[3] A.G. Lee, Lipid–protein interactions in biological membranes: a structural perspective, Biochim. Biophys. Acta 1612 (2003) 1–40.
[4] E. Posse, A. Vinals, B. de Arcuri, R. Farias, R.D. Morero, Lysozyme induced fusion of negatively charged phospholipid vesicles, Biochim. Biophys. Acta 104 (1990) 390–394.
[5] K. Arnold, D. Hoekstra, S. Ohki, Association of lysozyme to phospholipid surfaces and vesicle fusion, Biochim. Biophys. Acta 1124 (1992) 88–94.
[6] E. Posse, B.F. DeArcuri, R.D. Morero, Lysozyme interactions with phospholipid vesicles: relationships with fusion and release of aqueous content, Biochim. Biophys. Acta. 1193 (1994) 101–106.
[7] B.F. de Arcuri, G.F. Vechetti, R.N. Chehin, F.M. Goni, R.D. Morero, Protein-induced fusion of phospholipid vesicles of heterogeneous sizes, Biochem. Biophys. Res. Commun. 262 (1999) 586–590.
[8] O. Zschornig, G. Paasche, C. Thieme, N. Korb, A. Fahrwald, K. Arnold, Association of lysozyme with phospholipid vesicles is accompanied by membrane surface dehydration, Gen. Physiol. Biophys. 19 (2000) 85–101.
[9] T. Tsunoda, T. Imura, M. Kadota, T. Yamazaki, H. Yamauchi, K. Ok Kwon, S. Yokoyama, H. Sakai, M. Abe, Effects of lysozyme and bovine serum albumin on membrane characteristics of dipalmitoylphosphatidylglycerol liposomes, Colloids Surf., B Biointerfaces 20 (2001) 155–163.
[10] O. Zschornig, G. Paasche, C. Thieme, N. Korb, K. Arnold, Modulation of lysozyme charge influences interaction with phospholipid vesicles, Colloids Surf., B Biointerfaces 42 (2005) 69–78.
[11] J.J. Bergers, M.H. Vingerhoeds, L. van Bloois, J.N. Herron, L.H. Jassen, M.J. Fisher, D. Crommelin, The role of protein charge in protein–lipid interactions. pH-dependent changes of the electrophoretic mobility of liposomes through adsorption of water-soluble, globular proteins, Biochemistry 32 (1993) 4641–4649.
[12] V.M. Ioffe, G.P. Gorbenko, Lysozyme effect on structural state of model membranes as revealed by pyrene excimerization studies, Biophys. Chemist. 114 (2005) 199–204.
[13] S. Adams, A.M. Higgins, R.A.L. Jones, Surface-mediated folding and misfolding of proteins at lipid/water interfaces, Langmuir 18 (2002) 4854–4861.
[14] G.P. Gorbenko, V.M. Ioffe, P.K.J. Kinnunen, Binding of lysozyme to phospholipid bilayers: evidence for protein aggregation upon membrane association, Biophys. J. 93 (2007) 140–153.
[15] H. Zhao, E.K.J. Tuominen, P.K.J. Kinnunen, Formation of amyloid fibers triggered by phosphatidylserine-containing membranes, Biochemistry 43 (2004) 10302–10307.
[16] H.R. Ibrahim, M. Yamada, K. Matsushita, K. Kobayashi, A. Kato, Enhanced bactericidal action of lysozyme to *Escherichia coli* by inserting a hydrophobic pentapeptide into its C terminus, J. Biol. Chem. 269 (1994) 5053–5063.
[17] A. Pellegrini, U. Thomas, N. Bramaz, S. Klauser, P. Hunziker, R. von Fellenberg, Identification and isolation of a bactericidal domain in chicken egg white lysozyme, J. Appl. Microbiol. 82 (1997) 372–378.
[18] H.R. Ibrahim, U. Thomas, A. Pellegrini, A helix–loop–helix peptide at the upper lip of the active site cleft of lysozyme confers potent antimicrobial activity with membrane permeabilization action, J. Biol. Chem. 276 (2001) 43767–43774.
[19] M. Stefani, Protein misfolding and aggregation: new examples in medicine and biology of the dark side of the protein world, Biochim. Biophys. Acta 1739 (2004) 5–25.
[20] G.P. Gorbenko, P.K.J. Kinnunen, The role of lipid–protein interactions in amyloid-type protein fibril formation, Chem. Phys. Lipids 141 (2006) 72–82.
[21] H.J. Lee, C. Choi, S.J. Lee, Membrane-bound á-synuclein has a high aggregation propensity and the ability to seed the aggregation of the cytosolic form, J. Biol. Chem. 277 (2002) 671–678.
[22] J. Molotkovsky, P. Dmitriev, I. Molotkovskaya, L. Bergelson, E. Manevich, Synthesis of new fluorescent phospholipids and a study of their behavior in model membranes, Bioorg.Khim. 7 (1981) 586–600.
[23] J. Molotkovsky, E. Manevich, E. Gerasimova, I. Molotkovskaya, V. Polessky, L. Bergelson, Differential study of phosphatidylcholine and sphingomyelin in human high-density lipoproteins with lipid-specific fluorescent probes, Eur. J. Biochem. 122 (1982) 573–579.

[24] J.R. Lakowicz, Principles of Fluorescent Spectroscopy, 2nd ed.Plenum Press, New York, 1999.
[25] A.A. Bulychev, V.N. Verchoturov, B.A. Gulaev, Current Methods of Biophysical Studies, Vyschaya shkola, Moscow, 1988.
[26] B.K. Fung, L. Stryer, Surface density determination in membranes by fluorescence energy transfer, Biochemistry 17 (1978) 5241–5248.
[27] G. Gorbenko, T. Handa, H. Saito, J. Molotkovsky, M. Tanaka, M. Egashira, M. Nakano, Effect of cholesterol on bilayer location of the class A peptide Ac-18A-NH2 as revealed by fluorescence resonance energy transfer, Eur. Biophys. J. 32 (2003) 703–709.
[28] R. Dale, J. Eisinger, W. Blumberg, The orientational freedom of molecular probes. The orientation factor in intramolecular energy transfer, Biophys. J. 26 (1979) 161–194.
[29] I. Boldyrev, X. Zhai, M.M. Momsen, H.L. Brockman, R.E. Brown, J.G. Molotkovsky, New BODIPY lipid probes for fluorescence studies of membranes, J. Lipid Res. 48 (2007) 1518–1532.
[30] T. Imoto, L.S. Forster, J.A. Rupley, F. Tanaka, Fluorescence of lysozyme: emission from tryptophan residues 62 and 108 and energy migration, Proc. Natl. Acad. Sci. U. S. A. 69 (1971) 1151–1155.
[31] E. Nishimoto, S. Yamashita, A.G. Szabo, T. Imoto, Internal motion of lysozyme studied by time-resolved fluorescence depolarization of tryptophan residues, Biochemistry 37 (1998) 5599–5607.
[32] L. Johansson, J. Molotkovsky, L. Bergelson, Fluorescence properties of anthrylvinyl lipid probes, Chem. Phys. Lipids 53 (1990) 185–189.
[33] B. Valeur, G. Weber, Resolution of the fluorescence excitation spectrum of indole into 1La- and 1Lb excitation bands, Photochem. Photobiol. 25 (1977) 441–444.
[34] B. Albinsson, M. Kubista, B. Norden, E. Thulstrup, Near-ultraviolet electronic transitions of the tryptophan fluorophore: linear dichroism, fluorescence anisotropy, and magnetic circular dichroism spectra of some indole derivatives, J. Phys. Chem. 93 (1989) 6646–6654.
[35] W.M. Yau, W. Wimley, K. Gawrisch, S. White, The preference of tryptophan for membrane interface, Biochemistry 37 (1998) 14713–14718.
[36] P. Polverino de Laureto, E. Frare, R. Gottardo, H. Van Dael, A. Fontana, Partly folded states of members of the lysozyme/lactalbumin superfamily: a comparative study by circular dichroism spectroscopy and limited proteolysis, Protein Sci. 11 (2002) 2932–2946.
[37] M. Mosior, S. McLaughlin, Electrostatics and reduction of dimensionality produce apparent cooperativity when basic peptides bind to acidic lipids in membranes, Biochim. Biophys. Acta 1105 (1992) 185–187.
[38] G. Denisov, S. Wanaski, P. Luan, M. Glaser, S. McLaughlin, Binding of basic peptides to membranes produces lateral domains enriched in the acidic lipids phosphatidylserine and phosphatidylinositol-4,5-bisphosphate: an electrostatic model and experimental results, Biophys. J. 74 (1998) 731–744.
[39] T. Heimburg, B. Angerstein, D. Marsh, Binding of peripheral proteins to mixed lipid membranes: effect of lipid demixing upon binding, Biophys. J. 76 (1999) 2575–2586.
[40] S. May, D. Harries, A. Ben-Shaul, Lipid demixing and protein–protein interactions in the adsorption of charged proteins on mixed membranes, Biophys. J. 79 (2000) 1747–1760.
[41] E.C. Mbamala, A. Ben-Shaul, S. May, Domain formation induced by the adsorption of charged proteins on mixed lipid membranes, Biophys. J. 88 (2005) 1702–1714.
[42] M.M. Sperotto, O.G. Mouritsen, Lipid enrichment and selectivity of integral membrane proteins in two-component lipid bilayers, Eur. Biophys. J. 22 (1993) 323–328.
[43] D. Haverstick, M. Glaser, Influence of proteins on the reorganization of phospholipid bilayers into large domains, Biophys. J. 55 (1989) 677–682.
[44] M.A. Carbone, P.M. Macdonald, Cardiotoxin II segregates phosphatidylglycerol from mixtures with phosphatidylcholine: 31P and 2H NMR spectroscopic evidence, Biochemistry 35 (1996) 3368–3378.
[45] C.M. Franzin, P.M. Macdonald, Polylysine-induced 2H NMR observable domains in phosphatidylserine/phosphatidylcholine lipid bilayers, Biophys. J. 81 (2001) 3346–3362.
[46] K. Gawrisch, J.A. Barry, L.L. Holte, T. Sinnwell, L.D. Bergelson, J.A. Ferretti, Role of interactions at the lipid–water interface for domain formation, Mol. Membr. Biol. 12 (1995) 83–88.
[47] S. Oellerich, S. Lecomte, M. Paternostre, T. Heimburg, P. Hildebrandt, Peripheral and integral binding of cytochrome *c* to phospholipids vesicles, J. Phys. Chem. 108 (2004) 3871–3878.
[48] Ye.A. Domanov, J.G. Molotkovsky, G.P. Gorbenko, Coverage-dependent changes of cytochrome *c* transverse location in phospholipid membranes revealed by FRET, Biochim. Biophys. Acta 1716 (2005) 49–58.
[49] M.J. Zuckermann, T. Heimburg, Insertion and pore formation driven by adsorption of proteins onto lipid bilayer membrane–water interfaces, Biophys. J. 81 (2001) 2458–2472.